

REVISION

25th June 2017

pH Effects on Molecular Hydrogen Storage in Porous Organic Cages Deposited onto Platinum Electrodes

Naiara Hernández-Ibáñez ¹, Jet-Sing M. Lee ², Jesus Iniesta ¹, Vicente Montiel Leguey ¹, Michael E. Briggs ², Andrew I. Cooper ², Elena Madrid ³, and Frank Marken*³

¹ *Departamento de Química física e Instituto Universitario de Electroquímica, Universidad de Alicante, Apartado 99, 03080 Alicante, Spain*

² *Department of Chemistry and Materials Innovation Factory, University of Liverpool, Crown Street, Liverpool L69 7ZD, UK*

³ *Department of Chemistry, University of Bath, Claverton Down, Bath BA2 7AY, UK*

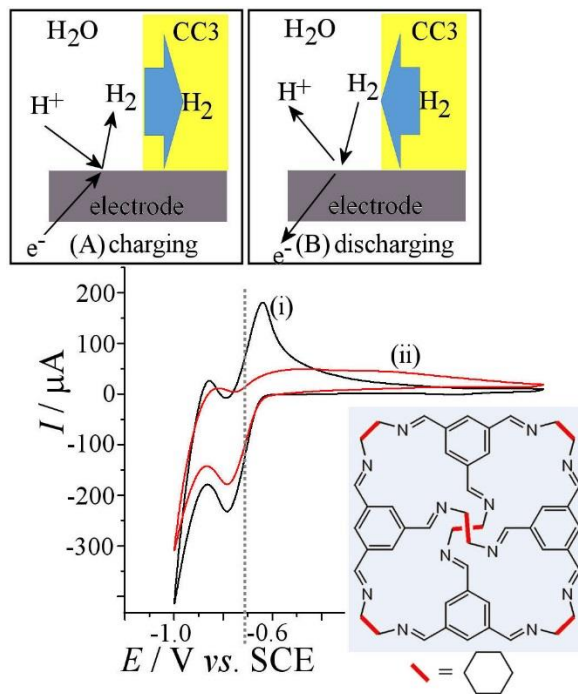
To be communicated to Journal of Electroanalytical Chemistry

(Special Issue Dedicated to Professor Roger Parsons)

Proofs to Frank Marken (f.marken@bath.ac.uk)

Abstract

Hydrogen absorption is a crucial process in energy storage (microscopic or macroscopic) and management and here a porous organic cage (POC) material is shown to bind and release hydrogen when deposited directly onto a platinum electrode and immersed into aqueous electrolyte. Preliminary voltammetry experiments for the POC **CC3** deposited onto a platinum disc electrode reveal uptake and release of hydrogen gas (probably coupled to water release and uptake, respectively) in the vicinity of the electrode. Significant pH effects on the rate of binding and release are reported and explained with a change in H_2 binding rate. In future, “wet” POCs or POCs dispersed in aqueous solution could be employed for enhancing hydrogen capture/transport in energy applications.



Graphical abstract:

Key words: hydrogen storage; fuel cells; water splitting; gas diffusion; clathrates; porous organic cages.

Introduction

Porous organic cages (POCs) are discrete, solution processible molecules that contain accessible, shape persistent cavities [1]. In the solid state they pack together to afford molecularly defined “open spaces” for the uptake/release of guest molecules [2,3]. Applications that take advantage of their well-defined pore structure, include gas and chiral separations [4,5], and chromatography [6], while dissolution in bulky solvents can result in the formation of porous liquids [7].

The porous organic cage **CC3** (see Figure 1 [8]) is an imine-linked [4+6] cage that is formed by the reaction of four molecules of 1,3,5-triformylbenzene with six molecules of homochiral 1,2-trans-cyclohexanediamine. **CC3** possesses tetrahedral symmetry and features four approximately triangular windows. In the solid state **CC3** preferentially packs with a window-to-window arrangement that results in an interconnected 3D diamondoid pore network. **CC3** has been reported to exhibit a nitrogen adsorption Brunauer–Emmett–Teller (BET) surface area of between 409 and 859 m²g⁻¹ [9], depending of the crystallinity of the sample. BET data also have shown the ability to bind hydrogen (H₂) gas into dry POC cages [8]. **CC3** only collapses upon reduction (hydrogenation of the imine to amine) and therefore the imine cage is shape persistent and always porous to provide a space for guest molecules. **CC3** is stable to boiling water (at neutral pH) for at least 4 h and has been shown to adsorb up to 20.1 wt% water reversibly [10], but **CC3** is somewhat sensitive to strongly alkaline and acidic environments, which make it unsuitable for conditions that substantially depart from neutrality [11]. Recently, proton conductivity was demonstrated

[12] with related POC molecules (where the imine was reduced to an amine) and it is interesting to further explore electrochemical properties and reactivity for these types of materials. Protonation of the POC **CC3** is likely to affect the ability to bind with guest molecules and when immersed into aqueous electrolyte, pH-dependent changes may be observed. Due to **CC3** being solid in neutral aqueous media, currently only estimates for the protonation characteristics are available.

Chemical Structure of **CC3**, $C_{72}H_{84}N_{12}$

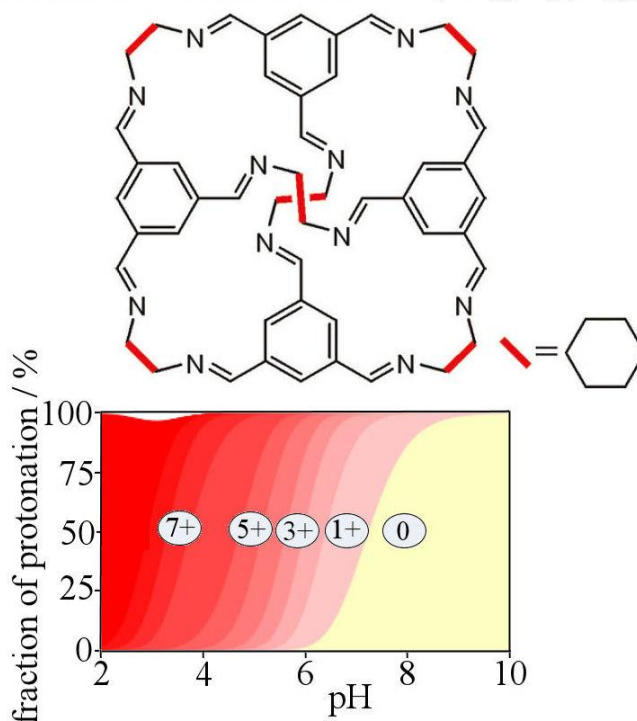


Figure 1. Molecular structure of **CC3** and estimated (ACDlabs Ltd. [13]) protonation sequence in aqueous environment. Note that **CC3** is chemically unstable outside of the neutral pH range from approximately pH 5-9 [10].

The estimated pK_{A1} for the first protonation is at $pH\ 7.2 \pm 0.4$. The plot in Figure 1 shows the sequence of further protonation equilibria up to the 7+ cation, by which time dissolution

and chemical degradation of the cage structure would almost certainly have started to occur [10]. This pK_A estimate does not take into account any structural effects introduced due to molecular interactions in the solid amorphous or crystalline state (or effects due to anions that are required to balance charge), but it provides an approximate value for the onset of protonation of **CC3** exposed to aqueous environments. The pH range from 5 to 9 appears to be the most interesting range.

Here, a preliminary investigation is reported of the behaviour of the solid **CC3** porous organic cage (as a representative case for a POC) as a deposit on a platinum electrode surface. The modified platinum electrode is immersed into aqueous buffer solutions and voltammetry is employed to study host/guest phenomena during hydrogen evolution. It can be assumed that the pH of the buffer solution is important and that protonation will occur from the surface of the **CC3** deposit possibly also progressing into the bulk of the porous material. It is shown that **CC3** has the ability to accumulate (store) molecular hydrogen in the solid state [8] and that the aqueous solution pH can be employed to modify the hydrogen binding rate and/or transport within the cage material. The voltammetric measurement can be employed as a screening tool for hydrogen binding into “wet” POCs and similar materials.

Experimental

Chemical Reagents

All solutions were prepared with doubly deionized water of resistivity not less than 18.2 M Ω cm⁻¹ (at 293 K) from a Thermo Scientific water purification system. Chloroform, phosphoric acid (85%), sodium dihydrogenphosphate (99%), and sodium phosphate dibasic hepta-hydrate were purchased from Sigma-Aldrich and used without further purification. CC3 was prepared following a literature procedure [8]. For pH studies 0.1 M aqueous solutions were prepared with the appropriate combination of sodium dihydrogenphosphate and sodium phosphate dibasic hepta-hydrate. For the solutions with pH upper 8 the pH was adjusted with aqueous NaOH.

Instrumentation

Electrochemical measurements were performed with a potentiostat system μ Autolab type III potentiostat/galvanostat (Metrohm Ltd.) controlled by Autolab GPES software version 4.9 for Windows XP. Experiments were performed in a conventional three electrode cell, with a Pt wire as a counter electrode, a KCl-saturated calomel reference (SCE, Radiometer, Copenhagen) as reference electrode, and a Pt disk electrode (BAS Ltd.) with 3 mm diameter as working electrode. The working electrode was modified by evaporation of a CC3 solution in chloroform (*vide infra*).

Procedures

Before use, the cleaning of the Pt electrode was performed by wet polishing with 0.3 μm alumina (Buehler Ltd.) on a polishing cloth followed by rinsing with copious amounts of water. Next, the Pt surface was electrochemically cleaned with 50 consecutive potential cycles from -0.2 V to +1.1 V vs. SCE (scan rate 0.1 V s⁻¹) in aqueous 0.5 M H₂SO₄ followed by rinsing. The working electrode was then prepared by drop-casting typically 4 μL of **CC3** solution (1 mg in 1 cm³ chloroform) onto the Pt electrode surface followed by solvent evaporation in air. Typical scanning electron micrographs for **CC3** deposits on platinum before and after electrochemistry are shown in Figure 2. The distribution of the **CC3** deposit can be seen to exhibit some non-uniformity. Importantly, **CC3** deposits are clearly observed as round patches of about 0.5 – 5.0 μm diameter both before and after electrochemical experiments.

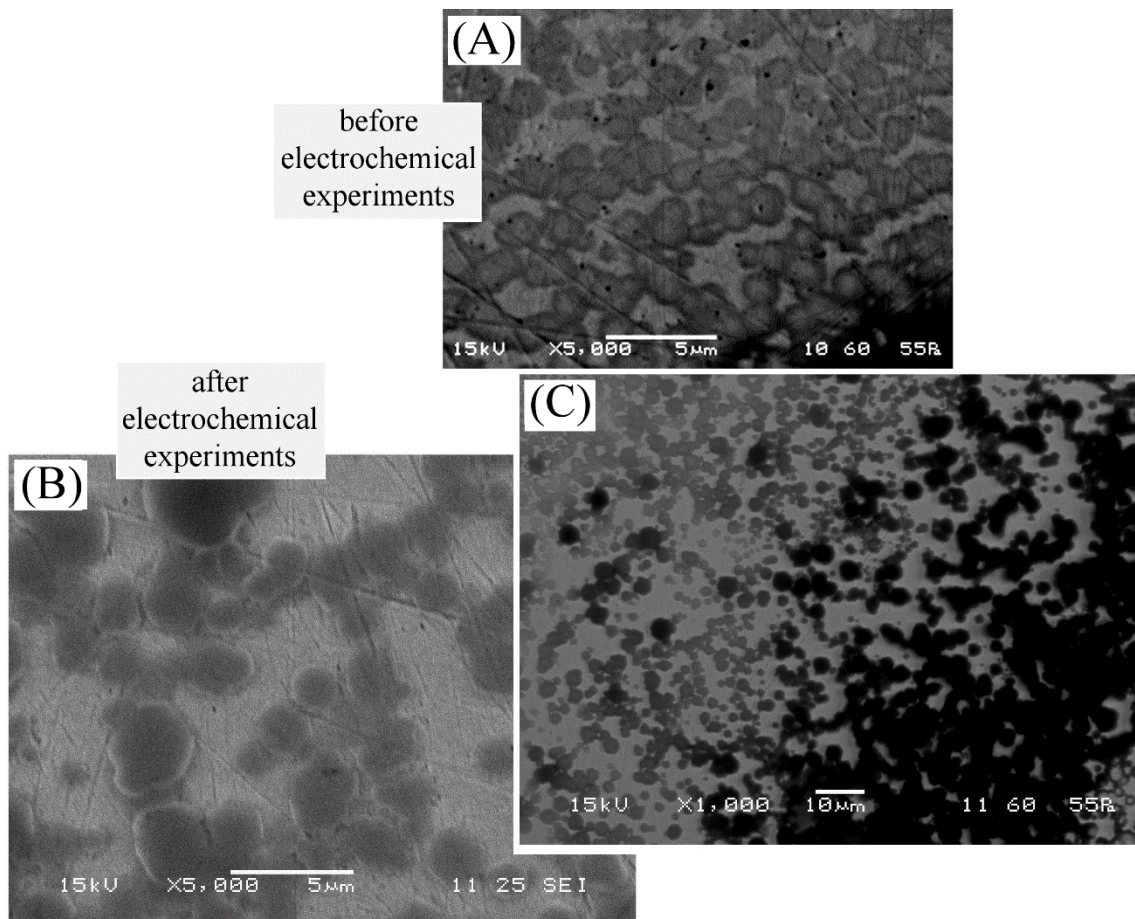


Figure 2. Scanning electron microscopy (SEM) images for a deposit of 4 µg CC3 on a 3 mm diameter Pt disc electrode before (A) and after electrochemistry (B,C).

Results and Discussion

Voltammetric Evidence for Hydrogen Storage in Porous Organic Cages

Deposits of CC3 on platinum are formed with globular shape (see Figure 2) rather than the usual octahedral crystal habit obtained from slowly crystallized CC3. In previous work [14] it has been shown that rapid precipitation of CC3 can result in loss of crystal habit and the introduction of defects, as a result of missing cages or crystal dislocations and grain boundaries. The original platinum surface is only partially blocked (see Figure 2), which is important for the reactivity of the electrode surface during the hydrogen evolution

reaction. The level of reactivity of the Pt | aqueous electrolyte interface versus the Pt | CC3 interface is currently not known, but the partial blocking of current at the electrode with CC3 deposit suggests that the main reaction zone here is at the Pt | aqueous electrolyte interface (Figure 3A,B).

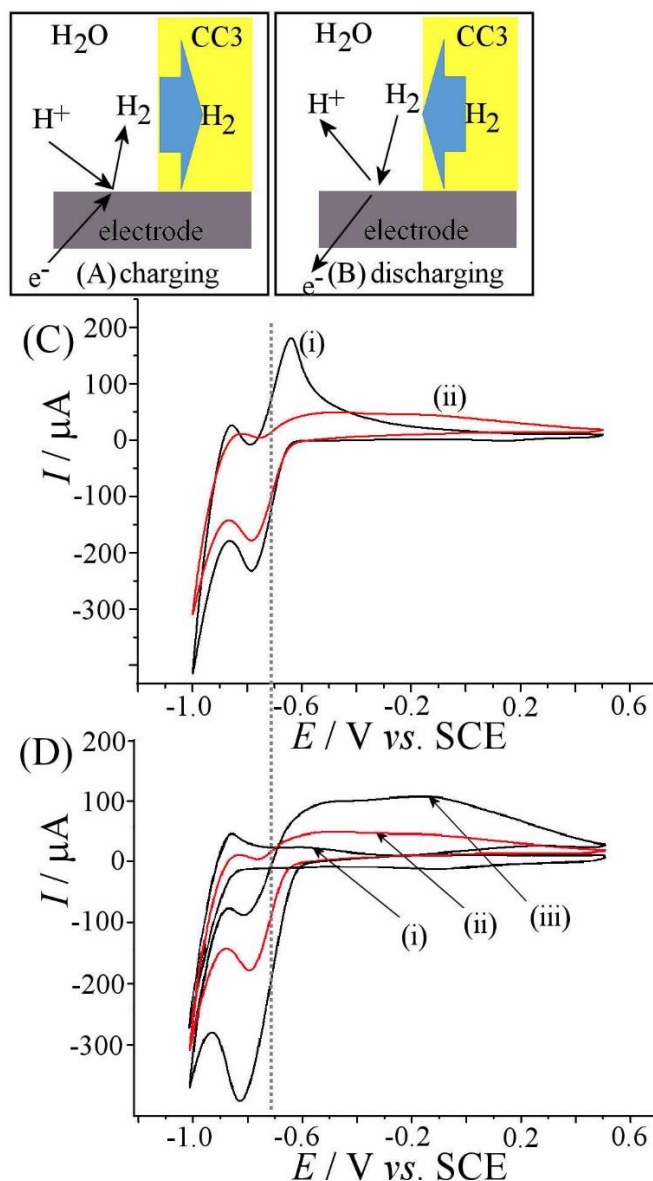


Figure 3. (A,B) Schematic drawing of the hydrogen evolution and hydrogen oxidation processes in the presence of CC3. (C) Cyclic voltammograms (scan rate 50 mVs⁻¹) for (i) 0 and (ii) 4 μg CC3 deposited onto a 3 mm diameter Pt disc electrode and immersed in aqueous 0.1 M phosphate buffer pH 7. (D) As above, but at (i) pH 11, (ii) pH 7.4, and (iii) pH 6.5.

Figure 3A and 3B show schematic drawings of the anticipated reactivity of protons being reduced to molecular hydrogen at the platinum electrode surface. Figure 3C shows experimental cyclic voltammetry data for (i) a bare platinum electrode and (ii) a **CC3**-coated platinum electrode. The reversible reduction process with midpoint potential $E_{\text{mid}} = \frac{1}{2} E_{\text{p,red}} + \frac{1}{2} E_{\text{p,ox}} = -0.75 \text{ V vs. SCE}$ is consistent with the reduction of the protons (from phosphate buffer anions HPO_4^{2-}) to molecular hydrogen, which is likely to occur under mixed diffusion and kinetic control. Due to the complexity of this process voltammetric data are interpreted and discussed here only for the hydrogen formation process (ignoring the kinetic effects in the proton reduction as well as any complexity that may arise from lack of supporting electrolyte around or within POC deposits or diffusion geometries). Electrode blocking effects that should arise from **CC3** deposits (see Figure 2) could be in part balanced out by non-planar diffusion but are also ignored at this time.

The cathodic formation of hydrogen at the platinum electrode surface leads to a local concentration c_{hydrogen} and diffusion away from the electrode. A hypothetical diffusion controlled anodic process with c_{hydrogen} in the bulk solution would lead to the same current peak except with hydrogen diffusion towards the electrode. This symmetry can be exploited to provide an estimate for c_{hydrogen} at the electrode surface. With the peak current for the re-oxidation peak, $I_{\text{peak}} \approx 200 \text{ } \mu\text{A}$, it is possible based on the Randles-Sevcik equation (equation 1 [15]) to estimate the concentration of molecular hydrogen generated

in the solution close to the electrode surface (as this would equal the value of $c_{hydrogen}$ for the hypothetical process involving diffusion of hydrogen to the surface).

$$I_{peak} = 0.446nFAC\sqrt{\frac{nFvD}{RT}} \quad (1)$$

Here, n denotes the number of electrons transferred per molecule diffusing to the electrode surface ($n = 2$ for H_2), F is the Faraday constant, A is the geometric electrode surface, v is the scan rate, D stands for $D_{hydrogen,water}$ the diffusion coefficient (for H_2 in water $4.5 \times 10^{-9} \text{ m}^2\text{s}^{-1}$ [16]), R is the gas constant, and T denotes the absolute temperature. Note that this equation is strictly valid for conditions of planar diffusion and reversible electron transfer, both of which may not be satisfied. The estimated concentration for hydrogen at the electrode surface in this case is 2.5 mM, which is not far from the solubility limit for hydrogen in water (ca. 0.8 mM at 293 K [17]). The local (close to the electrode) partial pressure of hydrogen can therefore be assumed to be close to atmospheric (1 bar) during hydrogen evolution.

With the **CC3** deposit applied, cyclic voltammograms are significantly different in shape (see Figure 3Cii). The proton reduction peak is approximately 20% lower in current indicative of partial electrode blocking. More importantly, the corresponding hydrogen oxidation peak is much lower (ca. 80% less current), which suggests that hydrogen has been removed from the solution. However, upon continuing the potential scan to higher potentials, at approximately 0.0 V vs. SCE a new and very broad oxidation peak response emerges indicative of release of molecular hydrogen. These results can be interpreted in

terms of a capture/release model (see Figure 3A and 3B) where **CC3** porous organic cages are able to remove the hydrogen from the aqueous phase with a delayed release as soon as the hydrogen is consumed again at the electrode surface. The shape of the voltammogram showing delayed release of hydrogen could be linked to either to capture and slow diffusion of hydrogen in solid **CC3** or capture and slow transfer kinetics across the **CC3** | aqueous electrolyte interface.

Data in Figure 3D show cyclic voltammograms recorded as a function of the solution pH. At pH 11 (which is outside of the range of stability for **CC3** but assumed here to not lead to decay of the solid within the timescale of the experiment) only the hydrogen evolution at the “solvent window” is observed with no significant sign of hydrogen storage under these conditions. At pH 7.4 clear evidence for “delayed” hydrogen oxidation is observed, which can be assigned to intermittent hydrogen storage in **CC3** cages. At pH 6.5 both the hydrogen production at the electrode (see reduction peak iii) as well as the broad hydrogen release signal are significantly enhanced. This may point to the fact that the pH can affect the hydrogen storage/release ability/kinetics of the **CC3** porous organic cages in wet conditions.

Chronoamperometric Analysis of Hydrogen Storage in Porous Organic Cages

In order to further examine the hydrogen uptake and release mechanism for porous organic cages deposited onto platinum electrode additional chronoamperometry experiments are performed. Figure 4A shows cyclic voltammetry data for (i) a bare electrode, (ii) 4 μg deposit, and (iii) 8 μg **CC3** deposit on platinum. As expected a higher amount of **CC3** on

the electrode surface cause additional “blocking” of the electrode surface and this causes a further decrease in the proton reduction peak. However, the broad oxidation peak for both 4 μg and 8 μg **CC3** appears similar. Appropriate potential limits for chronoamperometry $E_{\text{low}} = -0.85$ V vs. SCE and $E_{\text{high}} = -0.40$ V vs. SCE are selected.

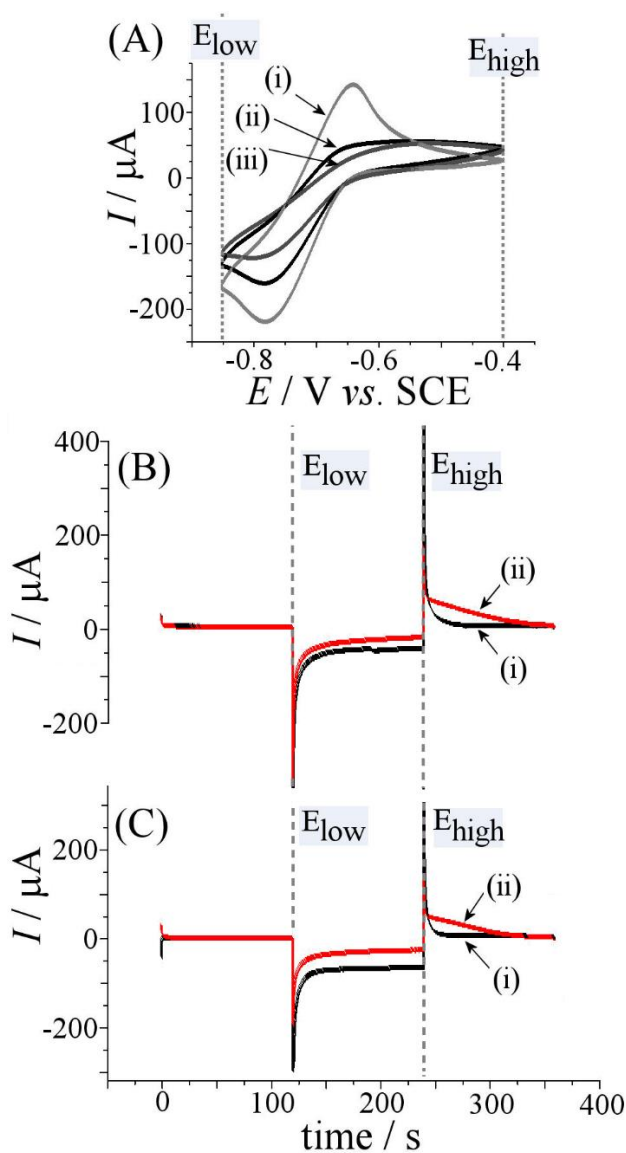


Figure 4. (A) Cyclic voltammograms (scan rate 50 mVs^{-1}) for (i) 0, (ii) 4, (iii) 8 μg **CC3** deposited onto a 3 mm diameter Pt disc electrode and immersed in aqueous 0.1 M phosphate buffer pH 7. (B) Chronoamperometry for (i) 0 and (ii) 4 μg **CC3** stepping the potential from $E_{\text{low}} = -0.85$ V vs. SCE to $E_{\text{high}} = -0.40$ V vs. SCE. (C) As above, but for (ii) 8 μg **CC3**.

Figure 4B shows chronoamperometry data for a pH 7 buffer solution and a 4 μg **CC3** deposit. The two traces show current at bare platinum (i) and current at **CC3** modified platinum (ii). During the reduction step, clearly less current flows in the presence of **CC3** due to partial blocking of the electrode surface. However, during the oxidation step the current at the bare platinum electrode decays rapidly (consistent with fast diffusion of molecular hydrogen into the aqueous solution phase) whereas a new broad oxidation process shows the release of hydrogen from the **CC3** deposit. The process only decays slowly over 60 seconds. When doubling the amount of **CC3** (see Figure 4C) the reduction of protons occurs with a slightly lower current, but the release of molecular hydrogen appears similar and over a similar period of time.

It is interesting to compare the integrated charge for reduction and oxidation as a measure of hydrogen capture efficiency. In theory, for a reversible electron transfer under conditions of planar diffusion, the ratio of anodic charge divided by cathodic charge (at a given time after applying the potential) should be 0.586 or 58.6 % [18]. For the bare platinum electrode over a period of 120 seconds a charge of 75 mC is generated and most of this can be assigned to hydrogen evolution followed by diffusional (and convective) loss of molecular hydrogen into the solution phase. The following oxidation allows 10 mC (or only 13%) of the hydrogen to be recovered. Due to the long duration of the experiment diffusional losses are enhanced by natural convection. In contrast, in the presence of 4 μg **CC3** a charge of 47 mC due to hydrogen generation (cathodic) is followed by 29 mC (or 61%) recovery (anodic). For a deposit of 8 μg **CC3** the reduction produces 44 mC hydrogen (cathodic)

and the oxidation suggests 22 mC (or 50%) recovery (anodic). Clearly, responses in the presence of **CC3** seem closer to the diffusional 58.6% [18] and hydrogen appears to be stored in the **CC3** porous organic cage material to prevent convective losses.

Effects of pH on Hydrogen Storage in Molecular Cages

With the chronoamperometry technique revealing the extent of the binding of molecular hydrogen into the porous molecular cages, it is interesting to explore effects of pH. Figure 5 shows data for aqueous 0.1 M phosphate buffer solution at pH 6, 7, 8, and 11 (which is beyond the range of chemical **CC3** stability, but employed here to contrast behaviour).

When comparing the release of hydrogen from **CC3** at pH 6 (Figure 5A) with pH 7 (Figure 5B) there seems to be a change in rate. At pH 6 the release seems to persist whereas at pH 7 the release seems to decay and stop after approximately 60 seconds. At pH 8 (Figure 5C) the release decays even faster after approximately 30 seconds. A better comparison of data is shown in Figure 5D for pH 6, 7, 8, and 11. Clearly, the release of hydrogen is higher and more sustained only at pH 6.

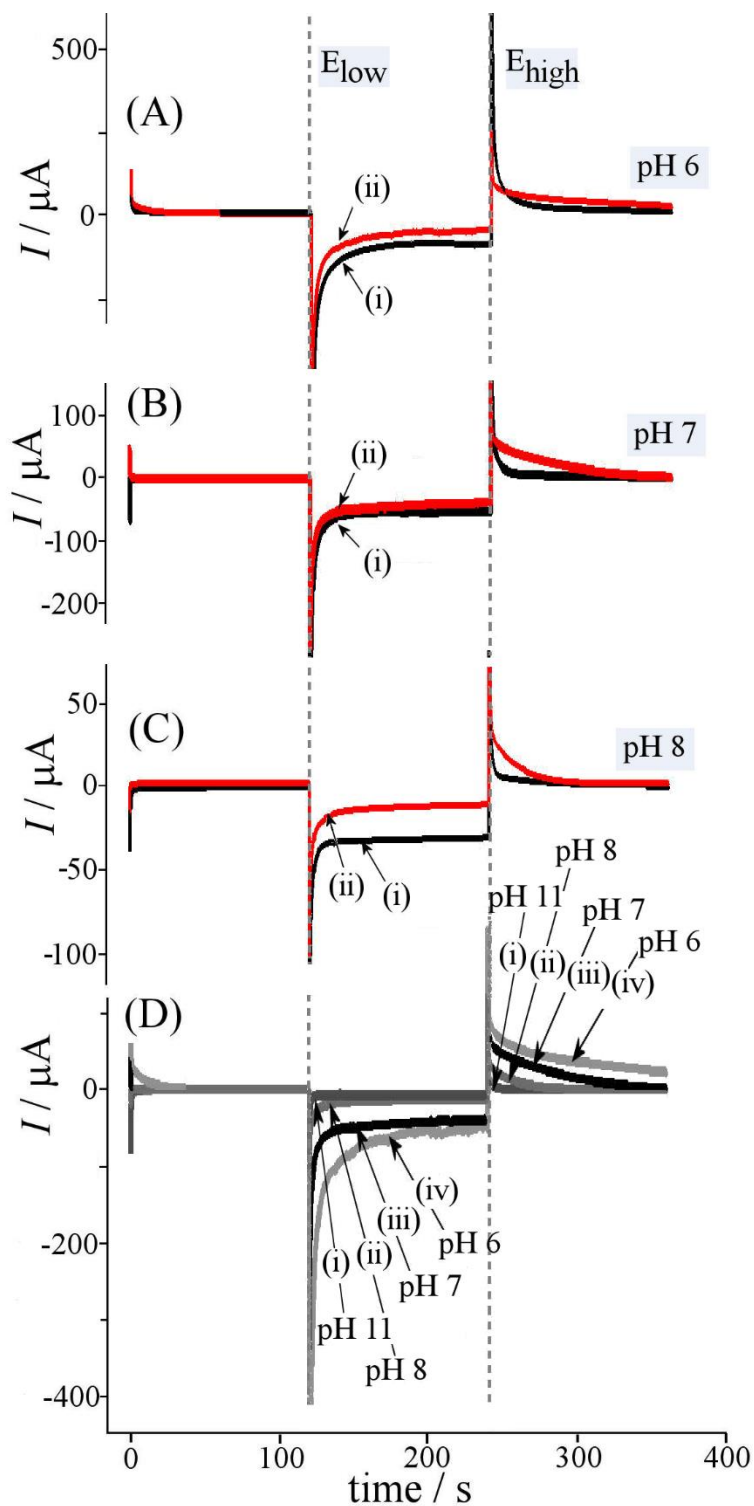


Figure 5. Chronoamperometry (stepping the potential from $E_{\text{low}} = -0.85$ V vs. SCE to $E_{\text{high}} = -0.40$ V vs. SCE) for $4 \mu\text{g}$ CC3 deposited onto a 3 mm diameter Pt disc electrode and immersed in aqueous 0.1 M phosphate buffer (A) pH 6, (B) pH 7, (C) pH 8, and (D) comparison for pH 6, 7, 8, and at 11 (outside the stability range).

For the interpretation of these effects one could compare the release time for the hydrogen during oxidation, τ , estimated as 120 s, 60 s, 30 s for pH 6, 7, and 8, respectively. Diffusion rates of hydrogen within the CC3 are unlikely to be affected by pH, but the release kinetics of hydrogen at the CC3 | aqueous electrolyte may be affected by interfacial protonation.

At the interface between aqueous electrolyte and **CC3** solid hydrogen diffusion has to occur from a region of high diffusivity (solution) into a region of lower diffusivity (**CC3** solid). Therefore, at the interface the local concentration $c_{\text{hydrogen,CC3}}$ will be higher compared to the hydrogen concentration in the aqueous electrolyte, $c_{\text{hydrogen,water}}$. The charge under the oxidation response in Figure 5Div can be estimated as 6.6 mC, which corresponds to approximately 3.4 nmol hydrogen. The solid state crystallographic density of **CC3** is 0.973 g cm^{-3} (molecular weight 1128 g mol^{-1} [8]), which is consistent with $0.863 \text{ mol dm}^{-3}$. The $4 \text{ }\mu\text{g}$ **CC3** deposit is equivalent to 3.5 nmol. Therefore the ratio of hydrogen guest molecules to **CC3** host molecules appears to be close to unity and the apparent concentration of hydrogen in **CC3** close to 0.8 mol dm^{-3} . The ambient molar volume for hydrogen in the gas phase is 0.04 mol dm^{-3} , which suggests that a gas capture/compression effect is possible. Therefore one or even several molecules of molecular hydrogen per **CC3** organic cage may be stored under these conditions. The replacement of water molecules from within **CC3** to the aqueous surroundings is likely to be important in this process. Further work (theory and experiment) will be necessary to further quantify the hydrogen transport, permeability, and uptake/release kinetics in terms of H_2 molecules per cage **CC3** in colloidal systems and as a function of pH/protonation.

Conclusion

In preliminary voltammetric and chronoamperometric experiments it has been shown that solid forms of the porous organic cage material **CC3** are able to capture and store molecular hydrogen in solid state and immersed in aqueous buffer media. The facile hydrogen capture and release process (observed voltammetrically at the surface of platinum electrodes) may be associated with water exchange and the process is shown to be pH dependent. The hydrogen release rate from solid **CC3** appeared to decrease when going from pH 8 to 6. It is therefore suggested that the buffer solution pH can be used to change the rate of uptake/release and interaction of molecular hydrogen with the **CC3** porous organic cage material. Being able to “compress” substantial amounts of hydrogen into “wet” porous organic cages will be of significant interest in energy technology. In future, it will be important to employ a wider range of techniques (e.g SECM, *in situ* spectroscopy, *in situ* diffraction etc.) to confirm the hydrogen storage effect as a function of particle size and to provide a more quantitative understanding of binding constant and transport rates.

Acknowledgement

N.H. and J.I. thank MINICINN, Spain (projects CTQ2013-48280-C3-3-R and CTQ2016-76231-C2-2-R (AEI/FEDER, UE)) for financial support and the University of Alicante for support for a PhD exchange visit. J.-S.M.L., M.E.B., and A.I.C. thank EPSRC (EP/H000925/1) for financial support

References

- [1] M.E. Briggs, A.I. Cooper, *Chem. Mater.* 29 (2017) 149 – 157.
- [2] D. Holden, K.E. Jelfs, A. Trewin, D.J. Willock, M. Haranczyk, A.I. Cooper, *J. Phys. Chem. C* 118 (2014) 12734 – 12743.
- [3] G. Zhang, M. Mastalerz, *Chem. Soc. Rev.* 43 (2014) 1934 – 1947.
- [4] T. Hasell, M. Miklitz, A. Stephenson, M.A. Little, S.Y. Chong, R. Clowes, L.J. Chen, D. Holden, G.A. Tribello, K.E. Jelfs, A.I. Cooper, *J. Amer. Chem. Soc.* 138 (2016) 1653 – 1659.
- [5] L.J. Chen, P.S. Reiss, S.Y. Chong, D. Holden, K.E. Jelfs, T. Hasell, M.A. Little, A. Kewley, M.E. Briggs, A. Stephenson, K.M. Thomas, J.A. Armstrong, J. Bell, J. Busto, R. Noel, J. Liu, D.M. Strachan, P.K. Thallapally, A.I. Cooper, *Nature Mater.* 13 (2014) 954 – 960.
- [6] A. Kewley, A. Stephenson, L.J. Chen, M.E. Briggs, T. Hasell, A.I. Cooper, *Chem. Mater.* 27 (2015) 3207 – 3210.
- [7] N. Giri, M.G. Del Pópolo, G. Melaugh, R.L. Greenaway, K. Rätzke, T. Koschine, L. Pison, M.F. Costa Gomes, A.I. Cooper, S.L. James, *Nature* 527 (2015) 216 – 220.
- [8] T. Tozawa, J.T.A. Jones, S.I. Swamy, S. Jiang, D.J. Adams, S. Shakespeare, R. Clowes, D. Bradshaw, T. Hasell, S.Y. Chong, C. Tang, S. Thompson, J. Parker, A. Trewin, J. Bacsa, A.M.Z. Slawin, A. Steiner, A.I. Cooper, *Nature Mater.* 8 (2009) 973 – 978.

-
- [9] T. Hasell, S.Y. Chong, K.E. Jelfs, D.J. Adams, A.I. Cooper, *J. Amer. Chem. Soc.* 134 (2012) 588 – 598.
- [10] T. Hasell, M. Schmidtman, C.A. Stone, M.W. Smith, A.I. Cooper, *Chem. Commun.* 48 (2012) 4689 – 4691.
- [11] M. Liu, M.A. Little, K.E. Jelfs, J.T.A. Jones, M. Schmidtman, S.Y. Chong, T. Hasell, A.I. Cooper, *J. Am. Chem. Soc.* 136 (2014) 7583 – 7586.
- [12] M. Liu, L.J. Chen, S. Lewis, S.Y. Chong, M.A. Little, T. Hasell, I.M. Aldous, C.M. Brown, M.W. Smith, C.A. Morrison, L.J. Hardwick, A.I. Cooper, *Nature Commun.* 7 (2016) 12750.
- [13] ACD/Labs Inc. accessed 10-01-2017 via <http://cds.rsc.org/>.
- [14] T. Hasell, J.L. Culshaw, S.Y. Chong, M. Schmidtman, M.A. Little, K.E. Jelfs, E.O. Pyzer-Knapp, H. Shepherd, D.J. Adams, G.M. Day, A.I. Cooper, *J. Am. Chem. Soc.* 136 (2014) 1438 – 1448.
- [15] A.J. Bard, L.R. Faulkner, *Electrochemical Methods*, 2nd ed., Wiley, New York, 2001, p. 231.
- [16] P.T.H.M. Verhallen, L.J.P. Oomen, A.J.J.M. Vanderelsen, A.J. Kruger, J.M.H. Fortun, *Chem. Engineer. Sci.* 39 (1984) 1535-1541.
- [17] *Handbook of Chemistry and Physics*, D.R. Lide, 94th ed., CRC Press, London, 1993, p. 6 – 3.
- [18] A.J. Bard, L.R. Faulkner, *Electrochemical Methods*, 2nd ed., Wiley, New York, 2001, p. 214.